Role of Reactive Halogen Species in Disinfection Byproduct Formation during Chlorine Photolysis

Devon Manley Bulman and Christina K. Remucal*

Read Online

ACCESS | Metrics & More | Article Recommendations | SI Supporting Information

ABSTRACT: The multiple reactive oxidants produced during chlorine photolysis effectively degrade organic contaminants during water treatment, but their role in disinfection byproduct (DBP) formation is unclear. The impact of chlorine photolysis on dissolved organic matter (DOM) composition and DBP formation is investigated using lake water collected after coagulation, flocculation, and filtration at pH 6.5 and pH 8.5 with irradiation at three wavelengths (254, 311, and 365 nm). The steady-state concentrations of hydroxyl radical and chlorine radical decrease by 38−100% in drinking water compared to ultrapure water, which is primarily attributed to radical scavenging by natural water constituents. Chlorine photolysis transforms DOM through multiple mechanisms to produce DOM that is more aliphatic in nature and contains novel high molecular weight chlorinated DBPs that are detected via high-resolution mass spectrometry. Quenching experiments demonstrate that reactive chlorine species are partially responsible for the formation of halogenated DOM, haloacetic acids, and haloacetonitriles, whereas trihalomethane formation decreases during chlorine photolysis. Furthermore, DOM transformation primarily due to direct photolysis alters DOM such that it is more reactive with chlorine, which also contributes to enhanced formation of novel DBPs during chlorine photolysis.
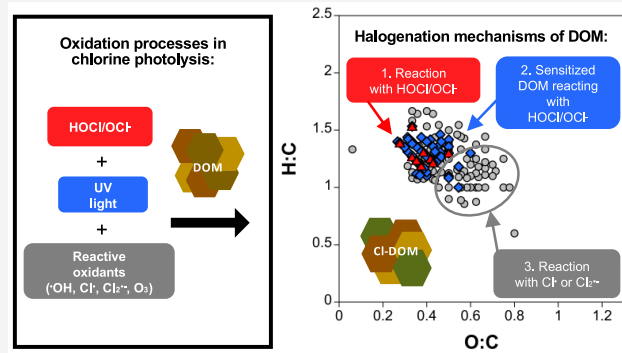
INTRODUCTION

Organic contaminants, including pharmaceuticals and pesticides, are found in drinking water sources[1−5] and present an unknown risk to human health.[4−6] Many of these compounds are not removed by traditional drinking water[7] or wastewater[8−10] treatment processes. As the impact of climate change becomes more profound, water scarcity will continue to increase, resulting in greater reliance on alternative water sources such as potable reuse options.[11]

Advanced oxidation processes (AOPs) such as chlorine[12−15] or hydrogen peroxide[14,16,17] photolysis are effective for oxidizing organic contaminants. These AOPs generate hydroxyl radical ($^\bullet OH$), a highly reactive and nonselective oxidant that reacts with most organic compounds.[12−15,18,19] Additionally, chlorine photolysis generates other reactive oxidants, including chlorine radical ($Cl^\bullet$), dichloride radical anion ($Cl_2^{\bullet-}$), and ozone (O_3), via homolytic cleavage of free available chlorine (i.e., the mixture of hypochlorous acid and hypochlorite, referred to here as chlorine; Supporting Information Schematic S1).[20−24] These reactive oxidants are scavenged by naturally occurring constituents in water such as organic and inorganic carbon,[14,21,25−27] resulting in lower oxidant steady-state concentrations. The effect of scavenging is thought to be greater for $^\bullet OH$ than for other oxidants[25,28,29] due to the greater reactivity of $^\bullet OH$ with organic and inorganic carbon.[27,30] Decreasing the reactive oxidant concentration will limit the efficacy of contaminant removal, highlighting the need for insight into radical scavenging during chlorine photolysis.

Halogenated disinfection byproducts (DBPs) form during the reaction of dissolved organic matter (DOM) with chlorine-based disinfectants[31−35] and are of concern due to potential carcinogenicity and other human health risks.[36−40] However, only nine organic DBPs are regulated in drinking water in the United States despite the identification of over 600 different halogenated organic compounds in drinking water treated with chlorine.[35−38,40−42] During DBP formation, chlorine, a strong electrophile,[43] preferentially reacts with electron-rich moieties within DOM.[34,44] These same electron-rich moieties may also be highly susceptible to reaction with reactive chlorine species, including $Cl^\bullet$ and $Cl_2^{\bullet-}$. Because $Cl^\bullet$ and $Cl_2^{\bullet-}$ can react by either electron transfer or chlorine addition,[45] it is possible that halogen radical reactions could lead to elevated DBP production during chlorine photolysis.

Targeted DBP formation during chlorine photolysis compared to chlorine alone ranges widely in past studies.[46] Generally, trihalomethanes (THMs) do not change or increase slightly during chlorine photolysis with low pressure UV light (LP UV; single-wavelength 254 nm light) compared to dark chlorination,[47−50] but increase with medium pressure UV light (MP UV; broad spectrum light ranging 200−400 nm)[47,51] and UV-A light.[48] Haloacetic acids (HAAs) decrease during chlorine photolysis with LP UV light,[47−49] but increase with MP UV and UV-A light.[47,48,51] Haloacetonitriles (HANs) increase during chlorine photolysis with both MP and LP UV light.[49,51,52] Despite these common trends, past studies do not yield a conclusive understanding of how the unique combination of chlorine, UV light, and reactive oxidants present in chlorine photolysis affect DBP formation.

High-resolution mass spectrometry methods such at Fourier transform-ion cyclotron resonance mass spectrometry (FT−ICR MS) can be used to investigate molecular-level changes in DOM and to identify high molecular weight halogenated organic compounds. Changes in DOM composition provide insight into how DOM may react in subsequent treatments (e.g., with residual disinfectant in the distribution system).[34,53] For example, previous investigation into DOM composition during conventional water treatment with FT−ICR MS found ~800 halogenated formulas postchlorination.[42] The formation of novel high molecular weight chlorinated formulas during chlorine photolysis has not yet been investigated.

All waters that might be treated by chlorine photolysis contain DOM, which may scavenge reactive oxidants and form DBPs. Therefore, understanding the impact of natural water constituents on oxidant production during chlorine photolysis, as well as the formation of both novel and known DBPs, is critical to applying the AOP in water treatment. Furthermore, the ability of reactive halogen species to form DBPs through halogen addition is a concern for chlorine photolysis, but this mechanism has not yet been shown experimentally in DOM. We combine bulk and molecular-level techniques to quantify oxidant scavenging and to investigate the transformation of dissolved organic matter during chlorine photolysis with UV-C light used in engineered applications and UV-B and UV-A light that is found in the solar spectrum. Additionally, we evaluate the role of multiple oxidative processes to provide mechanistic insight into halogenated disinfection byproduct formation during chlorine photolysis.

■ MATERIALS AND METHODS

Materials. Sodium hypochlorite was standardized using a Shimadzu UV−visible spectrometer ($\epsilon_{292} = 365$ M^{-1} cm^{-1}).[22] All other compounds were used as received (Section S1). Water samples (treated Mendota water, TMW) were collected from a pilot-scale drinking water treatment plant in the Water Science and Engineering Laboratory (University of Wisconsin—Madison) in which water from eutrophic Lake Mendota undergoes alum coagulation/flocculation, sedimentation, and dual-media filtration.[54] Samples were further filtered through a 0.2 μm filter before storing at 4 °C. This sample was selected because it is representative of a treated surface water (Table S1). The first TMW sample (March 8, 2019) was used for all experiments except the sequential treatment experiments, in which a second TMW sample (TMW2, October 31, 2019) was used due to sample volume limitations.

Sample Treatments. All experiments were conducted with 10 mM phosphate (pH 6.5) or borate (pH 8.5) buffer. The pH values were selected to fall above and below the acid dissociation constant of chlorine (pK_a = 7.5).[22] All solutions were brought to room temperature and were in equilibrium with the atmosphere. The initial chlorine concentration in chlorinated samples was 4 mg-Cl$_2$/L. The chlorine demand of TMW was <0.5 mg-Cl$_2$/L over the experimental duration (Figure S2). Photolysis experiments were conducted in a Rayonet merry-go-round photoreactor with either four 254 ± 1 nm bulbs, sixteen 311 ± 22 nm bulbs, or sixteen 365 ± 10 nm bulbs (Section S2).[20] 254 nm is representative of LP UV irradiation used during water treatment. The longer wavelengths are emitted by medium pressure UV lamps (200−400 nm)[20] and are found in the solar spectrum, making them relevant for solar applications.[20,21,55] Sample treatment times of six (254 nm), five (311 nm), and 30 min (365 nm) were selected to normalize total chlorine loss.

TMW samples were treated with dark chlorination, direct photolysis, chlorine photolysis, or quenched chlorine photolysis. Quenched chlorine photolysis samples contained 6 mM tert-butanol (t-BuOH), which scavenges >98% $^{\bullet}$OH and Cl$^{\bullet}$ and decreases [O$_3$] by 20−30% by scavenging O(^{3}P).[21] Residual chlorine was quenched with sodium thiosulfate.[20,56]

Analytical Methods. Dissolved organic carbon concentrations ([DOC]) were measured using a total organic carbon analyzer (Section S4). Anions were quantified using ion chromatography. Specific UV absorbance at 254 nm (SUVA$_{254}$) was calculated as the ratio of the absorbance at 254 nm to [DOC].[57]

Reactive oxidants were quantified using nitrobenzene ($^{\bullet}$OH), benzoate ($^{\bullet}$OH, Cl$^{\bullet}$, and Cl$_2^{\bullet-}$), and cinnamic acid (O$_3$) as probe compounds as described previously.[20] Free available chlorine was quantified using 1,3,5-trimethoxybenzene.[58] All probe compounds were quantified using high-performance liquid chromatography (Section S4).

Targeted DBPs including THMs (chloroform, bromoform, bromodichloromethane, and dibromochloromethane), HAAs (bromochloroacetic acid, bromodichloroacetic acid, chlorodibromoacetic acid, dibromoacetic acid, dichloroacetic acid, monobromoacetic acid, monochloroacetic acid, tribromoacetic acid, and trichloroacetic acid), and HANs (bromochloroacetonitrile, dibromoacetonitrile, dichloroacetonitrile, and trichloroacetonitrile) were quantified using EPA methods 551.1 (THMs and HANs)[59] and 552.2 (HAAs; Section S6).[60]

High-Resolution Mass Spectrometry. Samples were prepared using solid-phase extraction after adjusting to pH < 2.5 with formic acid[61−63] and analyzed by FT−ICR MS (SolariX XR 12T) using negative mode electrospray ionization. Molecular formulas with C$_{0−80}$H$_{0−140}$O$_{0−80}$N$_{0−1}$S$_{0−1}$P$_{0−1}$Cl$_{0−3}$^{13}C$_{0−1}$ and a mass error <0.5 ppm were allowed after internal calibration.[64−66] All masses matched to chlorine-containing formulas were required to have a ^{37}Cl isotopologue. Bulk DOM properties including H:C$_w$, O:C$_w$, and carbon-normalized double bond equivalents (DBE/C$_w$) were calculated as relative intensity-weighted averages from the assigned molecular formulas in each sample. Details on instrumental settings and data processing are provided in Sections S7 and S8.

Sequential Treatment. Sequential treatment experiments to investigate the impact of direct photolysis and reaction with $^{\bullet}$OH on DOM reactivity were conducted with the TMW2
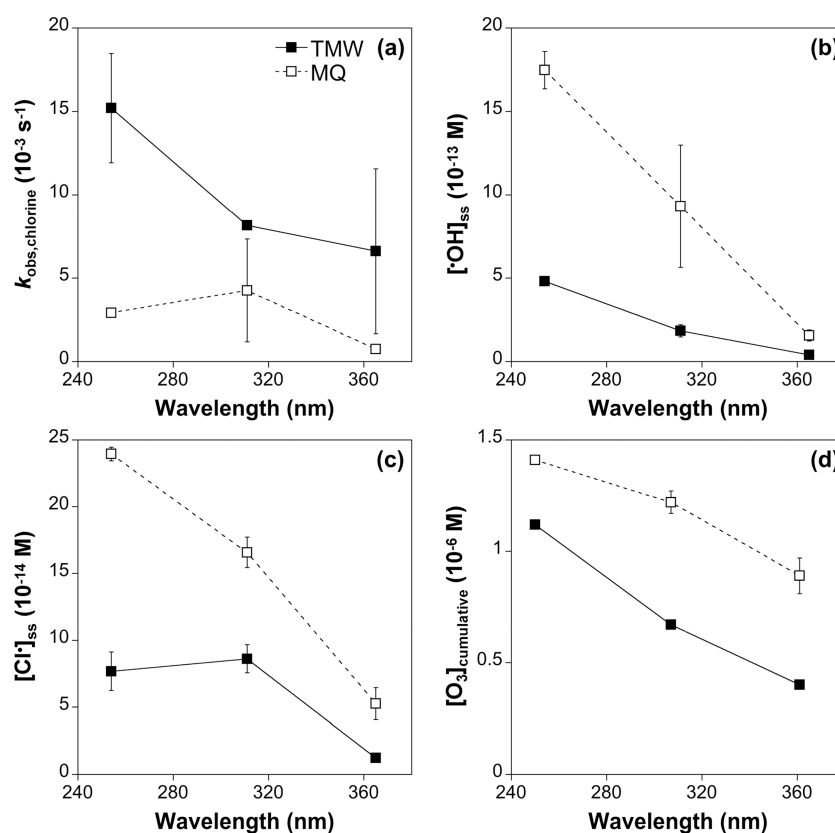
Figure 1. (a) Observed chlorine loss rate constant, (b) hydroxyl radical steady-state concentration, (c) chlorine radical steady-state concentration, and (d) cumulative ozone concentration as a function of wavelength at pH 6.5 in Milli-Q water (MQ) and treated Mendota water (TMW) during chlorine photolysis.

sample (Section S9). Hydroxyl radical control samples were generated using UV/H_2O_2 at 254 nm.[14] $[H_2O_2]_{initial}$ was 40 μM in order to achieve the same hydroxyl radical steady-state concentration as the chlorine photolysis treatment (Figure S15) and excess H_2O_2 was quenched with sodium thiosulfate.[67] Sequential treatment samples at pH 6.5 were treated with irradiation or UV/H_2O_2 for 6 min followed by 6 min of dark chlorination (4 mg-Cl_2/L), which was analogous to the chlorine photolysis treatment time. Samples were extracted and analyzed by FT–ICR MS.

RESULTS AND DISCUSSION

Effect of Natural Water Constituents on Reactive Oxidants. DOM and inorganic constituents can decrease contaminant removal during chlorine photolysis by consuming chlorine, scavenging reactive oxidants, or limiting oxidant production through light screening. The importance of these processes is investigated by quantifying the observed chlorine loss rate constant ($k_{obs,chlorine}$) and oxidant concentrations at pH 6.5 and 8.5 with 254, 311, and 365 nm irradiation in buffered Milli-Q water and in treated Lake Mendota water (Table S1). The chlorine loss rate constant is higher in TMW than in Milli-Q water under nearly all conditions (Figures 1a and S1a), with the exception of one sample due to the high molar absorptivity of OCl^- at pH 8.5 and 311 nm.[20] The increase in $k_{obs,chlorine}$ is not attributable to chlorine demand during the short experimental time scales (Figure S2a). Additionally, light screening is minimal as the same trends are observed when the data is corrected for light screening (Figure S1f; Table S2). Therefore, the increase in $k_{obs,chlorine}$ in

natural water is attributed to radical chain reactions involving carbon-centered radicals, which is similarly responsible for increases in $k_{obs,chlorine}$ in the presence of model compounds (e.g., methanol).[68] This conclusion is supported by the greater relative increase in $k_{obs,chlorine}$ at shorter wavelengths where radical steady-state concentrations are higher (Figures 1 and S1), allowing for more radical-induced chlorine loss.

$^\bullet$OH is a desirable oxidant in AOPs because it reacts with most organic contaminants of interest.[29,69,70] However, the nonselectivity of $^\bullet$OH means that it is scavenged by natural water constituents. $^\bullet$OH steady-state concentrations ($[^\bullet OH]_{ss}$) are 38.4 to 80.3% lower in TMW compared to Milli-Q water under all conditions tested (Figures 1b and S1b; Table S4). Higher $[^\bullet OH]_{ss}$ is observed at low pH and shorter wavelengths, in agreement with past work in the absence of DOM.[13,14,20,22,71] $^\bullet$OH scavenging in natural waters is primarily due to organic and inorganic carbon,[13,27,72] and branching ratio calculations demonstrate that >93% of carbon-scavenged $^\bullet$OH reacts with DOM (Table S5). Chloride reacts rapidly with $^\bullet$OH ($\sim$10^9 M^{-1} s^{-1}) to form $HOCl^{\bullet-}$,[73−77] but the rapid reverse reaction ensures that there is no net scavenging by Cl^-.[78−80] Note that $[^\bullet OH]_{ss}$ during photolysis of natural water constituents (e.g., DOM, NO_2^-) is an order of magnitude lower than $[^\bullet OH]_{ss}$ during chlorine photolysis (Figure S2d).

Reactive chlorine species (RCS) can degrade organic contaminants during chlorine photolysis (Schematic S1) and are scavenged by natural water constituents.[13,45] $[Cl^\bullet]_{ss}$ decreases 48 to 100% in TMW compared to Milli-Q water (Figures 1c and S1c; Table S4), with 72−77% of the carbon-
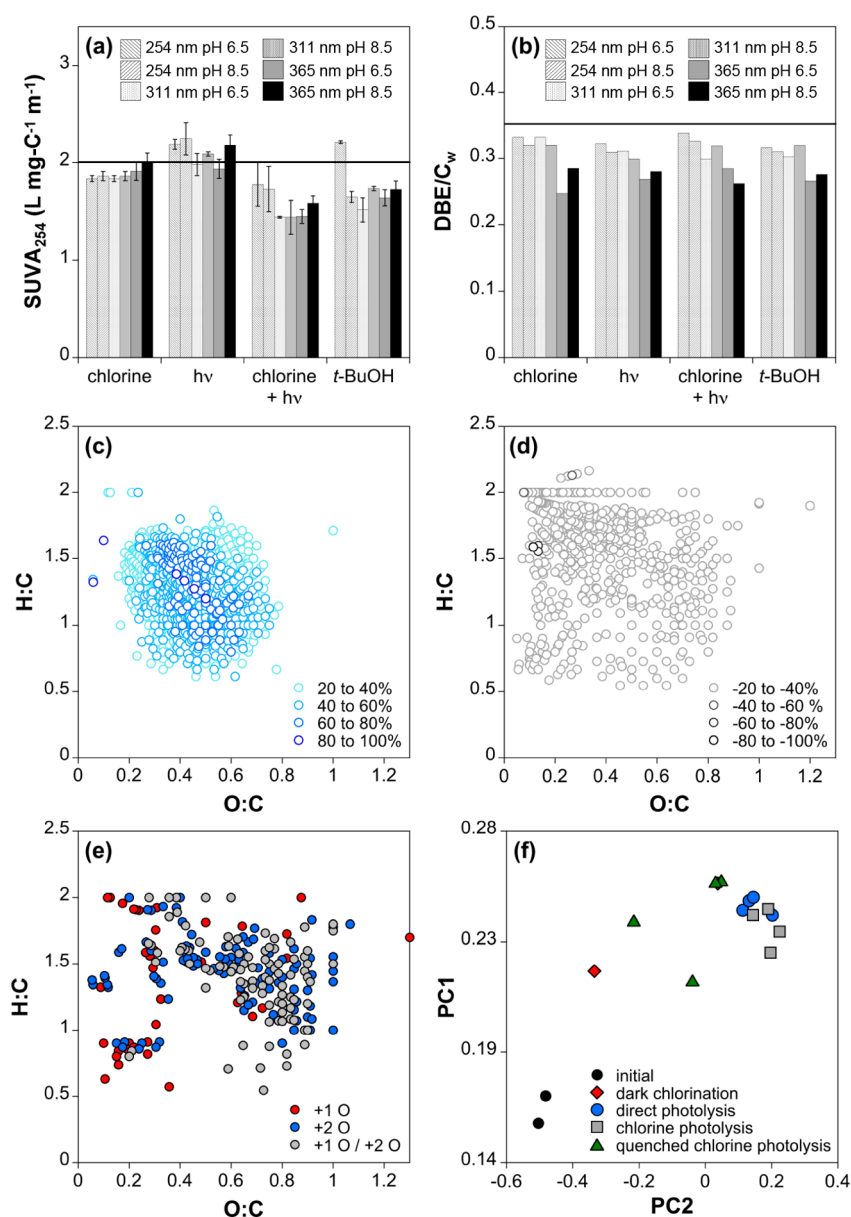
Figure 2. (a) SUVA$_{254}$ and (b) intensity weighted double bond equivalents per carbon (DBE/C$_w$) grouped by treatment at pH 6.5 and 8.5 and 254, 311, and 365 nm. Solid lines represent the initial values of SUVA$_{254}$ and DBE/C$_w$, respectively. van Krevelen diagrams of formulas common to the initial and all treated samples (pH 6.5 and 254, 311, and 365 nm) that (c) decrease or (d) increase in relative intensity during chlorine photolysis. Color corresponds to the percent change. Note that nearly all points in panel (d) fall within the −20 to −40% range. (e) van Krevelen diagram of oxygen addition formulas found after chlorine photolysis that are +1O (red), + 2O (blue), or either +1O or +2O (gray) from a formula in the initial sample. (f) Principal component analysis of the initial and treated samples at 254 and 311 nm, pH 6.5 and 8.5.

scavenged Cl$^\bullet$ attributable to HCO$_3^-$. Furthermore, the forward rate constant for the reaction of Cl$^\bullet$ with Cl$^-$ is faster than the reverse reaction, suggesting that additional scavenging by Cl$^-$ is possible.[27,30,73−77,81]

The reaction of Cl$^\bullet$ with Cl$^-$ produces Cl$_2^{\bullet-}$ (Schematic S1). [Cl$_2^{\bullet-}$]$_{ss}$ is 3 orders of magnitude higher than [Cl$^\bullet$]$_{ss}$ at low pH for all wavelengths in TMW, but is below the detection limit in Milli-Q water (Figure S1e). Cl$_2^{\bullet-}$ is a selective oxidant and typically reacts with organic contaminants at a lower rate constant than Cl$^\bullet$.[13,27,45] Conversion of Cl$^\bullet$ to Cl$_2^{\bullet-}$ is proportional to [Cl$^-$]; therefore, contaminant removal during chlorine photolysis will be more efficient at lower [Cl$^-$] for compounds that do not react with Cl$_2^{\bullet-}$.[20,45,76,77,82]

Ozone is produced during chlorine photolysis under the three irradiation conditions considered here,[20,55] but the impact of natural water constituents on its production has not been considered. The cumulative concentration of ozone is greater in Milli-Q water (i.e., (8.9−21.7) × 10^{-7} M vs (4.0−14.2) × 10^{-7} M in TMW; Figures 1d and S1d). [O$_3$] decreases with wavelength at low pH, while the opposite is true at high pH due to the higher molar absorptivity of OCl$^-$ than HOCl at high wavelengths and the more efficient formation of O(^{3}P), the O$_3$ precursor, from OCl$^-$.[20,21] Literature measurements similarly range from 4.0 × 10^{-7} M to 2.2 × 10^{-6} M in Milli-Q water,[20,21] with higher O$_3$ concentrations observed at high pH (Schematic S1).[20,23] The cumulative O$_3$ concentration decreases by 20.6 to 54.7%

in TMW compared to Milli-Q water (Figures 1d and S1d; Table S4). Reported rate constants for O_3 and DOM are $\sim10^3$ L mg-C^{-1} s^{-1},[83,84] while reaction rate constants between O_3 and inorganic water constituents are low (Table S8).[83−86] Therefore, we attribute the decrease in cumulative $[O_3]$ to scavenging by DOM (Table S7), which likely occurs through highly reactive phenolic moieties.[83,84,87]

Transformation of Dissolved Organic Matter. Understanding DOM transformation during chlorine photolysis provides insight into mechanisms of reaction during water treatment.[28,88] For example, the composition of DOM determines its DBP formation potential.[34,89−91] Therefore, changes in DOM composition during chlorine photolysis through a combination of direct photolysis, dark chlorination, or reaction with reactive oxidants might alter its reactivity with chlorine in distribution systems.[88,91,92] DOM composition following dark chlorination, direct photolysis, chlorine photolysis, and chlorine photolysis with a radical scavenger is investigated using UV−visible spectroscopy and high-resolution mass spectrometry to identify how chlorine, light, and reactive oxidants contribute to DOM alteration.

The dissolved organic carbon concentration reflects the total amount of carbon, whereas optical properties provide insight into DOM composition. For example, $SUVA_{254}$ is proportional to aromaticity.[57] The initial TMW sample has a low $[DOC]$ (i.e., 1.71 mg-C/L) as a result of the treatment plant processing. There is no evidence of mineralization during chlorine photolysis (Table S14), consistent with previous observations at pH 6.2 and 254 nm.[28] The initial TMW sample has a $SUVA_{254}$ value of 2.01 L mg-C^{-1} m^{-1}, indicating that the DOM is relatively aliphatic, as expected due to high microbial productivity in eutrophic lakes (Figure 2a).[65,66]

Dark chlorination and chlorine photolysis result in consistent decreases in $SUVA_{254}$ under all tested conditions, while direct photolysis results in a small increase or no change in $SUVA_{254}$ (Figure 2a; Table S14). A decrease in $SUVA_{254}$ during dark chlorination is expected because chlorine reacts preferentially with electron-rich compounds (e.g., aromatic moieties).[43] The largest decreases in $SUVA_{254}$ (i.e., 11.4−28.4%) are observed during chlorine photolysis which may be attributable to reaction of $^{\bullet}OH$ and RCS with aromatic DOM moieties.[45,46] The addition of t-BuOH during chlorine photolysis limits the effect on $SUVA_{254}$, with values decreasing 16.4% on average during quenched chlorine photolysis compared to 22.0% during chlorine photolysis. These observations suggest that reactive oxidants and direct reaction with HOCl/OCl⁻ contribute to the degradation of aromatic DOM, with minimal changes due to direct photolysis.

FT−ICR MS analysis is used to investigate molecular changes in DOM. An average of 2722 formulas are assigned to the initial and treated TMW samples (Table S13). Bray−Curtis dissimilarity and principal component analysis (PCA) compare similarity of DOM composition in all samples. Bray−Curtis dissimilarity analysis shows that treated samples group together (Figure S7). Similarly, PCA shows all treated samples clustering separately from initial samples. Additionally, PCA reveals that chlorine photolysis-treated samples group separately from the other treatments at 254 and 311 nm, while quenched chlorine photolysis samples fall in between chlorine photolysis and dark chlorination samples (Figure 2f). It is noteworthy that quenching radical species results in

DOM transformation that is different than either dark chlorination or direct photolysis alone.

As with $SUVA_{254}$, FT−ICR MS results demonstrate the loss of aromaticity with all treatments. Carbon-normalized double bond equivalents increase proportionally to aromaticity, while $H:C_w$ increases as the DOM becomes more aliphatic. DBE/C_w decreases and $H:C_w$ increases in all treated conditions relative to the initial sample (Figures 2b and S5a). Decreases in aromaticity are expected for all treatments because electron-rich aromatic systems are more reactive with chlorine and with radical species, resulting in possible ring cleavage products, and light is more readily absorbed by aromatic pi systems.[28,93−95] Interestingly, the decrease in aromaticity does not vary with treatment type at the molecular level, but does vary with pH. For all treatments and wavelengths, DBE/C_w decreases more at pH 6.5 compared to pH 8.5. For dark chlorination, this change is attributable to the higher reactivity of HOCl than OCl⁻ and is most pronounced with longer reaction times (365 nm; Figure 2b).[43] During chlorine photolysis, the change in DBE/C_w is attributable to the higher production of radicals at low pH (Figure 1), along with the combined effects of direct photolysis and reaction with HOCl.

The decrease in aromaticity during chlorine photolysis is further demonstrated by evaluating the change in intensity of molecular formulas found in both the initial and treated samples. Formulas that decrease in intensity during chlorine photolysis are aromatic (low H:C) and reduced (low O:C) and are tightly clustered in the lignin- and tannin-like regions of the van Krevelen diagram (Figure 2c).[96−98] These reactive formulas are similar across all considered treatments (Figure S9), highlighting the selective nature of light, chlorine, and reactive oxidants for aromatic, electron-rich compounds. In contrast, formulas that increase in intensity and are possible reaction products are widely distributed across the van Krevelen diagram with clear differences between treatments (Figure S10). In particular, formulas in the high O:C region only increase in relative intensity during chlorine photolysis (Figure 2d), which may be attributable to oxygen addition due to radical reactions with phenolic moieties.[13,27,30,45,68] Quenching the radical species during chlorine photolysis prevents the increase in intensity in this region (Figure S10d).

$O:C_w$ is a proxy for DOM oxidation state and is expected to increase with treatment because dark chlorination, direct photolysis, and chlorine photolysis are all oxidative processes. However, $O:C_w$ only increases during chlorine photolysis at low pH and wavelength when enough radical species are generated to sufficiently oxidize DOM (Figure S5b). Under all other conditions, $O:C_w$ decreases with treatment. Reaction with light, chlorine, and reactive oxidant species occurs in lower H:C (i.e., aromatic) formulas with a wide range of O:C values (Figure S9), producing formulas that are generally more aliphatic in nature (Figure S10). With the exception of chlorine photolysis (i.e., when high O:C formulas could be produced by O-addition due to $^{\bullet}OH$ reactions;[88,99] Figure 2d), the product formulas are generally lower in O:C and may be attributable to double-bond attack/ring cleavage reactions characteristic of reaction with $^{\bullet}OH$ and RCS (Figure S10).[45,46,100,101]

Oxidation is further investigated at the molecular level by considering the addition of 1 or 2 oxygen atoms to molecular formulas found in the initial sample. This analysis requires that oxygen addition products are only found after treatment
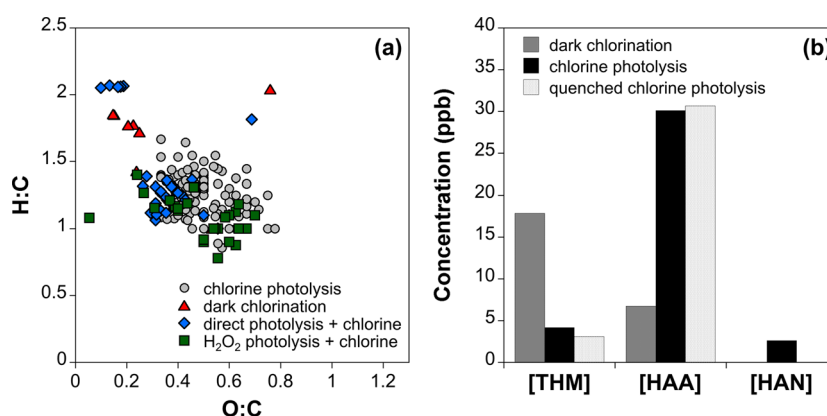
Figure 3. (a) CHOCl formulas formed during dark chlorination, chlorine photolysis, and sequential treatments in the second treated Mendota water sample (254 nm, pH 6.5). (b) Concentration of THMs, HAAs, and HANs during dark chlorination, chlorine photolysis, and quenched chlorine photolysis at 254 nm, pH 6.5.

and it is possible that a single product may be attributable to a + 1O or +2O reaction (Section S8). Chlorine photolysis results in the formation of >210 oxygen addition products localized in the high O:C region of the van Krevelen diagram (Figures 2e and S14; Table S16). Fewer oxygen-addition products are formed in quenched samples (130 on average), suggesting that reactive oxidants such as $^{\bullet}OH$ and O_3 contribute to oxygen-addition as expected based on their known reactivity with model compounds.[29,86] Therefore, there is evidence of oxidation at the molecular level during chlorine photolysis despite the decrease in $O:C_w$ at high pH and wavelengths (Figure S5b).

Formation of Halogenated Dissolved Organic Matter. FT−ICR MS enables the identification of chlorinated formulas, which can be considered as novel, high molecular weight disinfection byproducts.[42,44,102] CHOCl formulas are absent in initial samples and in samples exposed only to light, but are found in all samples treated with chlorine (Figure S11; Table S13). Dark chlorination results in up to 9 CHOCl formulas, with more CHOCl formulas formed at low pH because HOCl is a stronger electrophile than OCl^-.[43] Fewer CHOCl formulas are identified than in previous dark chlorination studies that had a longer disinfectant contact time, higher [DOC], acidification with hydrochloric acid rather than formic acid, and a less conservative approach to matching CHOCl formulas.[42,102] CHOCl formulas formed during dark chlorination are primarily in the lignin- and tannin-like regions of the van Krevelen diagram (Figures 3a and S11), which is consistent with previous observations of preferential chlorine reactivity with low H:C formulas in the same regions.[44,98] These CHOCl formulas are formed in the same region as formulas shown to be reactive during chlorination (Figure S9).

More CHOCl formulas are formed during chlorine photolysis than dark chlorination, with an average of 84 CHOCl formulas across the six chlorine photolysis treatment conditions (Table S13). The addition of t-BuOH as a quencher decreases the average number of CHOCl formulas under most chlorine photolysis conditions (i.e., low pH and wavelength; Figures S11a−c) to an average of 57, which is higher than the number observed during dark chlorination. However, quenching does not affect the formation of CHOCl formulas at pH 8.5 and 311 or 365 nm irradiation where radical concentrations are lower (Figures S11d−f; Table S13). The CHOCl formulas that are prevented by quenching are

attributable to reaction of reactive chlorine species (i.e., $Cl^{\bullet}$ and/or $Cl_2^{\bullet-}$) with DOM directly via chlorine addition,[45] demonstrating that RCS partially contribute to the formation of chlorinated DOM. The chlorinated formulas attributed to RCS halogenation are in the high O:C, low H:C region of the van Krevelen diagram (Figure S11a) where aromatic rings with hydroxy and methoxy substitution, along with other electron rich moieties, fall. These types of compounds are known to have high reactivity with $Cl^{\bullet}$ and $Cl_2^{\bullet-}$.[13,45] However, the inability of t-BuOH to prevent enhanced halogenation of DOM indicates that other processes, such as DOM transformation and subsequent changes in reactivity, may also impact elevated DOM chlorination during chlorine photolysis.

It is noteworthy that some of the novel DBPs contain nitrogen due to the increased toxicity of nitrogen-containing DBPs.[103,104] Fifteen distinct CHON formulas are formed during chlorine photolysis or quenched chlorine photolysis that contain either 1 or 2 chlorine atoms (Table S15), but are absent in control samples as well as samples treated by dark chlorination or UV irradiation. These formulas are found primarily at low pH and in greater abundance during chlorine photolysis in the absence of t-BuOH, suggesting that reactive chlorine species contribute to the formation of high molecular weight N-DBPs.

Impact of DOM Transformation on Organohalogenation. Chlorine photolysis involves a combination of light, chlorine, and multiple reactive oxidants that alter DOM composition. While the quenching experiments demonstrate that RCS contribute to direct halogenation of DOM, we hypothesized that alteration of DOM (e.g., via direct photolysis or reaction with nonhalogenating oxidants) could make DOM more susceptible to dark chlorination. For example, phenolic products produced by $^{\bullet}OH$ attack could make DOM more reactive; this mechanism has been proposed for model compounds (e.g., nitrobenzene and benzoate), but has not been considered in DOM.[22,68,105] Thus, we conducted a series of sequential experiments that exposed treated Mendota water to oxidation via UV/H_2O_2 (i.e., a source of $^{\bullet}OH$) or direct photolysis followed by dark chlorination (Section S9). $[^{\bullet}OH]_{ss}$ in the UV/H_2O_2 experiment was equivalent to the value measured during chlorine photolysis (Figure S15). These experiments used a second Mendota water sample (TMW2) so small differences are observed in

the initial water chemistry (Table S1). These experiments were conducted at pH 6.5 with 254 nm irradiation because these conditions generate the highest $[^\bullet OH]_{ss}$ and $[Cl^\bullet]_{ss}$ (Figure 1).

DOM transformation from direct photolysis and reaction with $^\bullet OH$ causes DOM to be more reactive toward chlorine, resulting in increased formation of CHOCl formulas (Figure 3a). A similar number of CHOCl formulas are found in both sequential samples (i.e., 32 CHOCl formulas in the direct photolysis-transformed sample and 27 in the UV/H$_2$O$_2$-transformed sample; Table S17), suggesting that UV photolysis is a major factor. The decrease in DBE/C$_w$ indicates that direct photolysis produces DOM that is, on average, more aliphatic. However, DOM photolysis also produces reactive intermediates that oxidize DOM moieties, as evidenced by the large number of oxygen addition formulas, making them more reactive with chlorine (Tables S16 and S17).[66,106,107] DOM sensitization by direct photolysis is further supported by the higher O:C ratio of CHOCl formulas compared to all matched formulas (Figure S6), which indicates preferential reactivity of chlorine with oxidized DOM. In contrast, only 4 CHOCl formulas are formed during dark chlorination for the same amount of time with no prior oxidation. As observed in the experiments conducted with TMW at two different pH values and three different wavelengths (Table S13), the most extensive halogenation (i.e., 124 formulas) is observed during chlorine photolysis. The increase in CHOCl formation in sequential treatment demonstrates that DOM is transformed via UV-mediated sensitization, making it more susceptible to direct reaction with chlorine. This mechanism accounts for CHOCl formulas formed during chlorine photolysis when RCS are quenched with t-BuOH. These results demonstrate that the combination of processes present during chlorine photolysis collectively contribute to enhanced halogenation, rather than simply direct reaction of RCS or chlorine.

Formation of Targeted Disinfection Byproducts. Halogenated DBPs present a known risk to human health and a subset of aliphatic DBPs (i.e., THMs and HAAs) are regulated in drinking water in the U.S.[36,37,41,42] Additionally, unregulated DBPs, such as halogenated aromatics, can have greater toxicity than regulated compounds.[35,38,40,108] This study focuses on the formation of THMs, HAAS, and HANs during chlorine photolysis to enable comparison with the conflicting literature on these DBPs. Previous investigations into the formation of these DBPs during chlorine photolysis are inconsistent, with some studies observing increased DBP formation compared to dark chlorination and other studies observing opposite trends.[47−52] These studies vary in water source, chlorine concentration, light source, and reaction time, making it challenging to draw clear conclusions.[46] We quantified the formation of four THMs, nine HAAs, and four HANs at two pH values and three wavelengths to investigate how pH and wavelength alter DBP formation in the same water sample with the same initial chlorine concentration.

The TMW sample did not contain any DBPs prior to treatment and DBPs are formed in all treatment conditions except direct photolysis (Tables S10−S12). Total THMs and HAAs (average of 12.5 μg/L and 12.6 μg/L, respectively) are formed during dark chlorination, whereas HANs are generally below the detection limit (Figures 3b and S4). There is no effect of sample pH on DBP formation despite the greater

reactivity of HOCl.[44] Treatment time is important, with more formation of all DBP classes at 30 min (i.e., used for comparison with 365 nm irradiation) than 5 min (i.e., used for comparison with 254 and 311 nm). This result is expected because DBP concentrations generally increase with contact time.[109]

THM formation decreases during chlorine photolysis compared to dark chlorination under most conditions. This trend is seen at both low and high pH, although the relative decrease in total THM concentration ([TTHM]) compared to dark chlorination is greater at high pH (Figures 3b and S4; Table S10). The decrease in [TTHM] during chlorine photolysis shows that the reactive oxidants produced during chlorine photolysis are less efficient at forming THMs than chlorine alone. It is likely that decreased chlorine contact time from chlorine degradation via photolysis and radical chain reactions,[50,55] along with the removal of aromatic precursors,[31,110,111] limits THM formation. Quenching $^\bullet OH$ and $Cl^\bullet$ with t-BuOH during chlorine photolysis has minimal effect on THM formation, further suggesting RCS are not involved in generating THMs (Table S10). These results are contrary to previous studies with higher initial chlorine concentrations and longer reaction times that showed an increase in THM formation during chlorine photolysis compared to dark chlorination.[47,51]

HAAs show the opposite trend as THMs and increase in concentration during chlorine photolysis relative to dark chlorination (Figures 3b and S4), which is consistent with previous studies at longer wavelengths.[47,48,51] Quenching radical species decreases HAA formation under most pH and wavelength combinations, although not down to the level of dark chlorination (Table S11). These data suggest that reactive chlorine species may contribute to the formation of HAAs. However, the increased formation of HAAs during chlorine photolysis may also be attributable to formation of HAA precursors from DOM transformation (i.e., as observed in the sequential experiments for novel DBP formation; Figure 3a) because quenching does not completely prevent the increased formation of HAAs.

HAN formation is greatest during chlorine photolysis compared to dark chlorination and quenched chlorine photolysis (Figures 3b and S4), in agreement with previous studies.[49,52] Only one sample for all pH and wavelength conditions had measurable HANs during radical quenching (i.e., 365 nm, pH 6.5; Table S12). The near complete inhibition of HAN formation during quenched chlorine photolysis indicates that HAN precursors are degraded during chlorine photolysis and suggests that enhanced formation of HANs is mediated by radical reactions, as observed for novel N-DBPs (Table S15).

Implications for Water Treatment. This study investigates the effect of natural water constituents on reactive oxidant concentrations and the effect of those oxidants on DOM transformation. The observed chlorine loss rate constant increases in the presence of DOM due to radical chain reactions (Figure 1a). Water with higher [DOC] will have enhanced $k_{obs,chlorine}$ in practical applications of chlorine photolysis. This effect is less pronounced at high pH and wavelength and is therefore less important in solar chlorine photolysis applications.

Natural water constituents are major radical scavengers and can decrease the efficacy of chlorine photolysis as an advanced oxidation process. Organic and inorganic carbon are the

primary sinks for reactive oxidants such as $^\bullet OH$ and $Cl^\bullet$, respectively, under our experimental conditions[13,27,30,72] and will lead to lower steady-state concentrations in natural waters. O_3 is more selective and less impacted by natural water constituents, suggesting that contaminants that react with ozone will be removed even in natural waters.

The alteration of DOM during chlorine photolysis has implications for DBP formation. DOM transformation during chlorine photolysis results in DOM that is more aliphatic and reduced as reactive, electron-rich DOM moieties are transformed, with the formation of oxygen addition products demonstrating oxidation at the molecular level (Figure 2). Importantly, the combination of oxidants (e.g., UV light and $^\bullet OH$) present during chlorine photolysis transforms DOM so that it is more reactive with chlorine, as shown using the sequential treatment experiments (Figure 3a). As a result, treatment systems that use chlorine photolysis may see increased formation of disinfection byproducts in the distribution system due to reaction of transformed DOM with residual disinfectant.

Furthermore, the analysis of DOM transformation by FT−ICR MS demonstrates that reactive chlorine species such as $Cl^\bullet$ and $Cl_2^{\bullet-}$ react with DOM via chlorine addition to form novel DBPs. This mechanism is demonstrated by the enhanced formation of CHOCl formulas during 254 and 311 nm chlorine photolysis and the ability of t-BuOH to limit the formation of some, but not all, of these formulas (Figure S11a−d). This is the first study to demonstrate the role of reactive chlorine species in forming high molecular weight halogenated DBPs, which could have implications for human health. The combination of RCS and DOM transformation also impacts the formation of targeted DBPs. THMs decrease during chlorine photolysis compared to dark chlorination due to consumption of chlorine. However, HAAs and HANs increase in concentration due to the formation of precursors from DOM transformation and from radical reactions. This study demonstrates that an understanding of multiple reaction pathways is necessary to mitigate DBP formation in this complex AOP.

ASSOCIATED CONTENT

Ⓢ Supporting Information

The Supporting Information is available free of charge at https://pubs.acs.org/doi/10.1021/acs.est.0c02039.

Details pertain to materials, analytical methods, water chemistry data, reactive oxidant quantification, FT−ICR MS data analysis, targeted DBP measurements, and sequential experimental design (PDF)

AUTHOR INFORMATION

Corresponding Author

Christina K. Remucal − Environmental Chemistry and Technology Program and Department of Civil and Environmental Engineering, University of Wisconsin—Madison, Madison, Wisconsin 53706, United States; ⓞ orcid.org/0000-0003-4285-7638; Phone: (608) 262-1820; Email: remucal@wisc.edu; Fax: (608) 262-0454

Author

Devon Manley Bulman − Environmental Chemistry and Technology Program, University of Wisconsin—Madison,

Madison, Wisconsin 53706, United States; ⓞ orcid.org/0000-0002-4999-9367

Complete contact information is available at:
https://pubs.acs.org/10.1021/acs.est.0c02039

Notes

The authors declare no competing financial interest.

REFERENCES

(1) Kolpin, D. W.; Furlong, E. T.; Meyer, M. T.; Thurman, E. M.; Zaugg, S. D.; Barber, L. B.; Buxton, H. T. Pharmaceuticals, hormones, and other organic wastewater contaminants in U.S. Streams, 1999−2000: A national reconnaissance. Environ. Sci. Technol. 2002, 36 (6), 1202−1211.

(2) Schwarzenbach, R. P.; Escher, B. I.; Fenner, K.; Hofstetter, T. B.; Johnson, C. A.; von Gunten, U.; Wehrli, B. The challenge of micropollutants in aquatic systems. Science 2006, 313 (5790), 1072−1077.

(3) Mompelat, S.; Thomas, O.; Le Bot, B. Contamination levels of human pharmaceutical compounds in french surface and drinking water. J. Environ. Monit. 2011, 13 (10), 2929−2939.

(4) Valcárcel, Y.; González Alonso, S.; Rodríguez-Gil, J. L.; Gil, A.; Catalá, M. Detection of pharmaceutically active compounds in the rivers and tap water of the Madrid region (Spain) and potential ecotoxicological risk. Chemosphere 2011, 84 (10), 1336−1348.

(5) Kostich, M. S.; Batt, A. L.; Lazorchak, J. M. Concentrations of prioritized pharmaceuticals in effluents from 50 large wastewater treatment plants in the U.S. and implications for risk estimation. Environ. Pollut. 2014, 184, 354−359.

(6) Stalter, D.; O'Malley, E.; von Gunten, U.; Escher, B. I. Fingerprinting the reactive toxicity pathways of 50 drinking water disinfection by-products. Water Res. 2016, 91, 19−30.

(7) Westerhoff, P.; Yoon, Y.; Snyder, S.; Wert, E. Fate of endocrine-disruptor, pharmaceutical, and personal care product chemicals during simulated drinking water treatment processes. Environ. Sci. Technol. 2005, 39 (17), 6649−6663.

(8) Fairbairn, D. J.; Arnold, W. A.; Barber, B. L.; Kaufenberg, E. F.; Koskinen, W. C.; Novak, P. J.; Rice, P. J.; Swackhamer, D. L. Contaminants of emerging concern: Mass balance and comparison of wastewater effluent and upstream sources in a mixed-use watershed. Environ. Sci. Technol. 2016, 50 (1), 36−45.

(9) Li, Z.; Sobek, A.; Radke, M. Fate of pharmaceuticals and their transformation products in four small European rivers receiving treated wastewater. Environ. Sci. Technol. 2016, 50 (11), 5614−5621.

(10) Stackelberg, P. E.; Furlong, E. T.; Meyer, M. T.; Zaugg, S. D.; Henderson, A. K.; Reissman, D. B. Persistence of pharmaceutical compounds and other organic wastewater contaminants in a conventional drinking-water-treatment plant. Sci. Total Environ. 2004, 329 (1−3), 99−113.

(11) Dong, S.; Page, M. A.; Massalha, N.; Hur, A.; Hur, K.; Bokenkamp, K.; Wagner, E. D.; Plewa, M. J. Toxicological comparison of water, wastewaters, and processed wastewaters. Environ. Sci. Technol. 2019, 53 (15), 9139−9147.

(12) Kwon, M.; Yoon, Y.; Kim, S.; Jung, Y.; Hwang, T.-M.; Kang, J.-W. Removal of sulfamethoxazole, ibuprofen and nitrobenzene by UV

and UV/chlorine processes: A comparative evaluation of 275 nm LED-UV and 254 nm LP-UV. *Sci. Total Environ.* **2018**, *637−638*, 1351−1357.

(13) Guo, K.; Wu, Z.; Shang, C.; Yao, B.; Hou, S.; Yang, X.; Song, W.; Fang, J. Radical chemistry and structural relationships of PPCP degradation by UV/chlorine treatment in simulated drinking water. *Environ. Sci. Technol.* **2017**, *51* (18), 10431−10439.

(14) Chuang, Y.-H.; Chen, S.; Chinn, C. J.; Mitch, W. A. Comparing the UV/monochloramine and UV/free chlorine advanced oxidation processes (AOPs) to the UV/hydrogen peroxide AOP under scenarios relevant to potable reuse. *Environ. Sci. Technol.* **2017**, *51* (23), 13859−13868.

(15) Hua, Z.; Guo, K.; Kong, X.; Lin, S.; Wu, Z.; Wang, L.; Huang, H.; Fang, J. PPCP degradation and DBP formation in the solar/free chlorine system: Effects of pH and dissolved oxygen. *Water Res.* **2019**, *150*, 77−85.

(16) Li, M.; Li, W.; Wen, D.; Bolton, J. R.; Blatchley, E. R.; Qiang, Z. Micropollutant degradation by the UV/H₂O₂ process: Kinetic comparison among various radiation sources. *Environ. Sci. Technol.* **2019**, *53* (9), 5241−5248.

(17) Miklos, D. B.; Hartl, R.; Michel, P.; Linden, K. G.; Drewes, J. E.; Hübner, U. UV/H₂O₂ process stability and pilot-scale validation for trace organic chemical removal from wastewater treatment plant effluents. *Water Res.* **2018**, *136*, 169−179.

(18) Yin, R.; Zhong, Z.; Ling, L.; Shang, C. The fate of dichloroacetonitrile in UV/Cl₂ and UV/H₂O₂ processes: Implications on potable water reuse. *Environ. Sci. Water Res. Technol.* **2018**, *4* (9), 1295−1302.

(19) Lu, X.; Shao, Y.; Gao, N.; Chen, J.; Deng, H.; Chu, W.; An, N.; Peng, F. Investigation of clofibric acid removal by UV/persulfate and UV/chlorine processes: Kinetics and formation of disinfection byproducts during subsequent chlor(am)ination. *Chem. Eng. J.* **2018**, *331*, 364−371.

(20) Bulman, D. M.; Mezyk, S. P.; Remucal, C. K. The impact of pH and irradiation wavelength on the production of reactive oxidants during chlorine photolysis. *Environ. Sci. Technol.* **2019**, *53* (8), 4450−4459.

(21) Forsyth, J. E.; Zhou, P.; Mao, Q.; Asato, S. S.; Meschke, J. S.; Dodd, M. C. Enhanced inactivation of *Bacillus subtilis* spores during solar photolysis of free available chlorine. *Environ. Sci. Technol.* **2013**, *47* (22), 12976−12984.

(22) Watts, M. J.; Linden, K. G. Chlorine photolysis and subsequent •OH radical production during UV treatment of chlorinated water. *Water Res.* **2007**, *41* (13), 2871−2878.

(23) Buxton, G. V.; Subhani, M. S. Radiation chemistry and photochemistry of oxychlorine ions. Part 1. Radiolysis of aqueous solutions of hypochlorite and chlorite ions. *J. Chem. Soc., Faraday Trans. 1* **1972**, *68*, 947−957.

(24) Buxton, G. V.; Subhani, M. S. Radiation chemistry and photochemistry of oxychlorine ions. Part 2. Photodecomposition of aqueous solutions of hypochlorite ions. *J. Chem. Soc., Faraday Trans. 1* **1972**, *68*, 958−969.

(25) Nowell, L. H.; Hoigné, J. Photolysis of aqueous chlorine at sunlight and ultraviolet wavelengths. 1. Degradation rates. *Water Res.* **1992**, *26* (5), 593−598.

(26) Buxton, G. V. Pulse radiolysis of aqueous solutions. Some rates of reaction of •OH and O•⁻ and pH dependence of the yield of O₃⁻. *Trans. Faraday Soc.* **1969**, *65*, 2150−2158.

(27) Fang, J.; Fu, Y.; Shang, C. The roles of reactive species in micropollutant degradation in the UV/free chlorine system. *Environ. Sci. Technol.* **2014**, *48* (3), 1859−1868.

(28) Varanasi, L.; Coscarelli, E.; Khaksari, M.; Mazzoleni, L. R.; Minakata, D. Transformations of dissolved organic matter induced by UV photolysis, hydroxyl radicals, chlorine radicals, and sulfate radicals in aqueous-phase UV-based advanced oxidation processes. *Water Res.* **2018**, *135*, 22−30.

(29) Buxton, G. V.; Greenstock, C. L.; Helman, W. P.; Ross, A. B. Critical review of rate constants for reactions of hydrated electrons, hydrogen atoms and hydroxyl radicals (•OH/O•⁻) in aqueous solution. *J. Phys. Chem. Ref. Data* **1988**, *17* (2), 513−886.

(30) Zhang, K.; Parker, K. M. Halogen radical oxidants in natural and engineered aquatic systems. *Environ. Sci. Technol.* **2018**, *52* (17), 9579−9594.

(31) Heller-Grossman, L.; Manka, J.; Limoni-Relis, B.; Rebhun, M. THM, haloacetic acids and other organic DBPs formation in disinfection of bromide rich sea of Galilee (Lake Kinneret) water. *Water Sci. Technol.: Water Supply* **2001**, *1* (2), 259−266.

(32) Agus, E.; Voutchkov, N.; Sedlak, D. L. Disinfection by-products and their potential impact on the quality of water produced by desalination systems: A literature review. *Desalination* **2009**, *237* (1−3), 214−237.

(33) Shah, A. D.; Mitch, W. A. Halonitroalkanes, halonitriles, haloamides, and *N*-nitrosamines: A critical review of nitrogenous disinfection byproduct formation pathways. *Environ. Sci. Technol.* **2012**, *46* (1), 119−131.

(34) Pifer, A. D.; Fairey, J. L. Suitability of organic matter surrogates to predict trihalomethane formation in drinking water sources. *Environ. Eng. Sci.* **2014**, *31* (3), 117−126.

(35) Yang, M.; Zhang, X.; Liang, Q.; Yang, B. Application of (LC/) MS/MS precursor ion scan for evaluating the occurrence, formation and control of polar halogenated DBPs in disinfected waters: A review. *Water Res.* **2019**, *158*, 322−337.

(36) Richardson, S. D.; Ternes, T. A. Water analysis: Emerging contaminants and current issues. *Anal. Chem.* **2011**, *83* (12), 4614−4648.

(37) Muellner, M. G.; Wagner, E. D.; Mccalla, K.; Richardson, S. D.; Woo, Y.-T.; Plewa, M. J. Haloacetonitriles vs. regulated haloacetic acids: Are nitrogen-containing DBPs more toxic? *Environ. Sci. Technol.* **2007**, *41* (2), 645−651.

(38) Plewa, M. J.; Wagner, E. D.; Richardson, S. D. TIC-tox: A preliminary discussion on identifying the forcing agents of DBP-mediated toxicity of disinfected water. *J. Environ. Sci.* **2017**, *58*, 208−216.

(39) Han, J.; Zhang, X. Evaluating the comparative toxicity of DBP mixtures from different disinfection scenarios: A new approach by combining freeze-drying or rotoevaporation with a marine polychaete bioassay. *Environ. Sci. Technol.* **2018**, *52* (18), 10552−10561.

(40) Richardson, S. D.; Ternes, T. A. Water analysis: Emerging contaminants and current issues. *Anal. Chem.* **2018**, *90* (1), 398−428.

(41) Jeong, C. H.; Wagner, E. D.; Siebert, V. R.; Anduri, S.; Richardson, S. D.; Daiber, E. J.; Mckague, A. B.; Kogevinas, M.; Villanueva, C. M.; Goslan, E. H.; Luo, W.; Isabelle, L. M.; Pankow, J. F.; Grazuleviciene, R.; Cordier, S.; Edwards, S. C.; Righi, E.; Nieuwenhuijsen, M. J.; Plewa, M. J. Occurrence and toxicity of disinfection byproducts in European drinking waters in relation with the HIWATE epidemiology study. *Environ. Sci. Technol.* **2012**, *46* (21), 12120−12128.

(42) Gonsior, M.; Schmitt-Kopplin, P.; Stavklint, H.; Richardson, S. D.; Hertkorn, N.; Bastviken, D. Changes in dissolved organic matter during the treatment processes of a drinking water plant in Sweden and formation of previously unknown disinfection byproducts. *Environ. Sci. Technol.* **2014**, *48* (21), 12714−12722.

(43) Acero, J. L.; Benitez, F. J.; Real, F. J.; Roldan, G. Kinetics of aqueous chlorination of some pharmaceuticals and their elimination from water matrices. *Water Res.* **2010**, *44* (14), 4158−4170.

(44) Lavonen, E. E.; Kothawala, D. N.; Tranvik, L. J.; Gonsior, M.; Schmitt-Kopplin, P.; Köhler, S. J. Tracking changes in the optical properties and molecular composition of dissolved organic matter during drinking water production. *Water Res.* **2015**, *85*, 286−294.

(45) Lei, Y.; Cheng, S.; Luo, N.; Yang, X.; An, T. Rate constants and mechanisms of the reactions of Cl• and Cl₂•⁻ with trace organic contaminants. *Environ. Sci. Technol.* **2019**, *53* (19), 11170−11182.

(46) Remucal, C. K.; Manley, D. Emerging investigators series: The efficacy of chlorine photolysis as an advanced oxidation process for drinking water treatment. *Environ. Sci. Water Res. Technol.* **2016**, *2* (4), 565−579.

(47) Liu, W.; Cheung, L. M.; Yang, X.; Shang, C. THM, HAA and CNCl formation from UV irradiation and chlor(am)ination of selected organic waters. *Water Res.* **2006**, *40* (10), 2033−2043.

(48) Pisarenko, A. N.; Stanford, B. D.; Snyder, S. A.; Rivera, S. B.; Boal, A. K. Investigation of the use of chlorine based advanced oxidation in surface water: Oxidation of natural organic matter and formation of disinfection byproducts. *J. Adv. Oxid. Technol.* **2013**, *16* (1), 137−150.

(49) Zhang, X.; Li, W.; Blatchley, E. R.; Wang, X.; Ren, P. UV/chlorine process for ammonia removal and disinfection by-product reduction: Comparison with chlorination. *Water Res.* **2015**, *68*, 804−811.

(50) Ben, W.; Sun, P.; Huang, C.-H. Effects of combined UV and chlorine treatment on chloroform formation from triclosan. *Chemosphere* **2016**, *150*, 715−722.

(51) Wang, D.; Bolton, J. R.; Andrews, S. A.; Hofmann, R. Formation of disinfection by-products in the ultraviolet/chlorine advanced oxidation process. *Sci. Total Environ.* **2015**, *518−519*, 49−57.

(52) Shah, A. D.; Dotson, A. D.; Linden, K. G.; Mitch, W. A. Impact of UV disinfection combined with chlorination/chloramination on the formation of halonitromethanes and haloacetonitriles in drinking water. *Environ. Sci. Technol.* **2011**, *45* (8), 3657−3664.

(53) Ding, S.; Deng, Y.; Bond, T.; Fang, C.; Cao, Z.; Chu, W. Disinfection byproduct formation during drinking water treatment and distribution: A review of unintended effects of engineering agents and materials. *Water Res.* **2019**, *160*, 313−329.

(54) Xagoraraki, I.; Harrington, G. W.; Assavasilavasukul, P.; Standridge, J. H. Removal of emerging waterborne pathogens and pathogen indicators by pilot-scale conventional treatment. *J. - Am. Water Works Assoc.* **2004**, *96* (5), 102−113.

(55) Sun, P.; Lee, W.-N.; Zhang, R.; Huang, C.-H. Degradation of DEET and caffeine under UV/chlorine and simulated sunlight/chlorine conditions. *Environ. Sci. Technol.* **2016**, *50* (24), 13265−13273.

(56) Willson, V. A. Determination of available chlorine in hypochlorite solutions by direct titration with sodium thiosulfate. *Ind. Eng. Chem., Anal. Ed.* **1935**, *7* (1), 44−45.

(57) Weishaar, J. L.; Aiken, G. R.; Bergamaschi, B. A.; Fram, M. S.; Fujii, R.; Mopper, K. Evaluation of specific ultraviolet absorbance as an indicator of the chemical composition and reactivity of dissolved organic carbon. *Environ. Sci. Technol.* **2003**, *37* (20), 4702−4708.

(58) Lau, S. S.; Dias, R. P.; Martin-Culet, K. R.; Race, N. A.; Schammel, M. H.; Reber, K. P.; Roberts, A. L.; Sivey, J. D. 1,3,5-Trimethoxybenzene (TMB) as a new quencher for preserving redox-labile disinfection byproducts and for quantifying free chlorine and free bromine. *Environ. Sci. Water Res. Technol.* **2018**, *4* (7), 926−941.

(59) Hodgeson, J. W.; Cohen, A. L.; Munch, D. J.; Hautman, D. P. *Method 551.1. Determination of Chlorination Disinfection Byproducts, Chlorinated Solvents, And Halogenated Pesticides/Herbicides in Drinking Water by Liquid−Liquid Extractions and Gas Chromatography with Electron Capture Detection*; U.S. Environmental Protection Agency: Cincinnati, 1995.

(60) Hodgeson, J. W.; Collins, J.; Barth, R. E.; Munch, D. J.; Munch, J. W.; Pawlecki, A. M. *Method 552.2 Determination of Haloacetic Acids and Dalapon in Drinking Water by Liquid−Liquid Extraction, Derivatization and Gas Chromatography with Electron Capture Detection*; U.S. Environmental Protection Agency: Cincinnati, 1995.

(61) Ziegler, G.; Gonsior, M.; Fisher, D. J.; Schmitt-Kopplin, P.; Tamburri, M. N. Formation of brominated organic compounds and molecular transformations in dissolved organic matter (DOM) after ballast water treatment with sodium dichloroisocyanurate dihydrate (DICD). *Environ. Sci. Technol.* **2019**, *53* (14), 8006−8016.

(62) Dittmar, T.; Koch, B.; Hertkorn, N.; Kattner, G. A simple and efficient method for the solid-phase extraction of dissolved organic matter (SPE-DOM) from seawater. *Limnol. Oceanogr.: Methods* **2008**, *6*, 230−235.

(63) Maizel, A. C.; Remucal, C. K. The effect of advanced secondary municipal wastewater treatment on the molecular composition of dissolved organic matter. *Water Res.* **2017**, *122*, 42−52.

(64) Koch, B. P.; Dittmar, T.; Witt, M.; Kattner, G. Fundamentals of molecular formula assignment to ultrahigh resolution mass data of natural organic matter. *Anal. Chem.* **2007**, *79* (4), 1758−1763.

(65) Maizel, A. C.; Li, J.; Remucal, C. K. Relationships between dissolved organic matter composition and photochemistry in lakes of diverse trophic status. *Environ. Sci. Technol.* **2017**, *51* (17), 9624−9632.

(66) Berg, S. M.; Whiting, Q. T.; Herrli, J. A.; Winkels, R.; Wammer, K. H.; Remucal, C. K. The role of dissolved organic matter composition in determining photochemical reactivity at the molecular level. *Environ. Sci. Technol.* **2019**, *53* (20), 11725−11734.

(67) Chu, W.; Gao, N.; Yin, D.; Krasner, S. W.; Mitch, W. A. Impact of UV/H$_2$O$_2$ pre-oxidation on the formation of haloacetamides and other nitrogenous disinfection byproducts during chlorination. *Environ. Sci. Technol.* **2014**, *48* (20), 12190−12198.

(68) Oliver, B. G.; Carey, J. H. Photochemical production of chlorinated organics in aqueous solutions containing chlorine. *Environ. Sci. Technol.* **1977**, *11* (9), 893−895.

(69) Bossmann, S. H.; Oliveros, E.; Göb, S.; Siegwart, S.; Dahlen, E. P.; Payawan, L.; Straub, M.; Wörner, M.; Braun, A. M. New evidence against hydroxyl radicals as reactive intermediates in the thermal and photochemically enhanced Fenton reactions. *J. Phys. Chem. A* **1998**, *102* (28), 5542−5550.

(70) Nowell, L. H.; Hoigné, J. Photolysis of aqueous chlorine at sunlight and ultraviolet wavelengths. 2. Hydroxyl radical production. *Water Res.* **1992**, *26* (5), 599−605.

(71) Yin, R.; Ling, L.; Shang, C. Wavelength-dependent chlorine photolysis and subsequent radical production using UV-LEDs as light sources. *Water Res.* **2018**, *142*, 452−458.

(72) Wols, B. A.; Hofman-Caris, C. H. M. Review of photochemical reaction constants of organic micropollutants required for UV advanced oxidation processes in water. *Water Res.* **2012**, *46* (9), 2815−2827.

(73) Grigor'ev, A. E.; Makarov, I. E.; Pikaev, A. K. Formation of Cl$_2$$^{\bullet-}$ in the bulk of solution during radiolysis of concentrated aqueous solutions of chlorides. *Khim. Vys. Energy* **1987**, *21* (2), 99−102.

(74) Jayson, G. G.; Parsons, B. J.; Swallow, A. J. Some simple, highly reactive, inorganic chlorine derivatives in aqueous solution. *J. Chem. Soc., Faraday Trans. 1* **1973**, *69*, 1597−1607.

(75) Kläning, U. K.; Wolff, T. Laser flash photolysis of HClO, ClO$^−$, HBrO, and BrO$^−$ in aqueous solution. Reactions of Cl$^−$ and Br$^−$ atoms. *Ber. Bunsen. Ges. Phys. Chem.* **1985**, *89*, 243−245.

(76) Nagarajan, V.; Fessenden, R. W. Flash photolysis of transient radicals. 1. X$_2$$^−$ with X = Cl, Br, I, and SCN. *J. Phys. Chem.* **1985**, *89* (11), 2330−2335.

(77) Yu, X.-Y.; Barker, J. R. Hydrogen peroxide photolysis in acidic aqueous solutions containing chloride ions. I. Chemical mechanism. *J. Phys. Chem. A* **2003**, *107* (9), 1313−1324.

(78) Wang, W.-L.; Wu, Q.-Y.; Huang, N.; Wang, T.; Hu, H.-Y. Synergistic effect between UV and chlorine (UV/chlorine) on the degradation of carbamazepine: Influence factors and radical species. *Water Res.* **2016**, *98*, 190−198.

(79) Gao, Y.-Q.; Gao, N.-Y.; Chen, J.-X.; Zhang, J.; Yin, D.-Q. Oxidation of β-blocker atenolol by a combination of UV light and chlorine: Kinetics, degradation pathways and toxicity assessment. *Sep. Purif. Technol.* **2020**, *231*, 115927.

(80) Dugan, H. A.; Summers, J. C.; Skaff, N. K.; Krivak-Tetley, F. E.; Doubek, J. P.; Burke, S. M.; Bartlett, S. L.; Arvola, L.; Jarjanazi, H.; Korponai, J.; et al. Long-term chloride concentrations in North American and European freshwater lakes. *Sci. Data* **2017**, *4*, 170101.

(81) Mertens, R.; von Sonntag, C. Photolysis (λ= 254 nm) of tetrachloroethene in aqueous solutions. *J. Photochem. Photobiol., A* **1995**, *85*, 1−9.

(82) Kläning, U. K.; Sehested, K.; Wolff, T. Laser flash photolysis and pulse radiolysis of iodate and periodate in aqueous solution. Properties of iodine (VI). *J. Chem. Soc., Faraday Trans. 1* **1981**, *77*, 1707–1718.

(83) von Sonntag, C.; von Gunten, U. *Chemistry of Ozone in Water and Wastewater Treatment*; IWA Publishing, 2012.

(84) Elovitz, M. S.; von Gunten, U.; Kaiser, H.-P. *The Influence of Dissolved Organic Matter Character on Ozone Decomposition Rates and R_{ct}*; Barrett, S. E.; Krasner, S. W.; Amy, G. L.; Eds.; ACS Publications: 2000.

(85) Dodd, M. C.; Buffle, M.-O.; von Gunten, U. Oxidation of antibacterial molecules by aqueous ozone: moiety-specific reaction kinetics and application to ozone-based wastewater treatment. *Environ. Sci. Technol.* **2006**, *40* (6), 1969–1977.

(86) von Gunten, U. Ozonation of drinking water: Part 1. Oxidation kinetics and products formation. *Water Res.* **2003**, *37*, 1443–1467.

(87) Hammes, F.; Salhi, E.; Köster, O.; Kaiser, H.-P.; Egli, T.; von Gunten, U. Mechanistic and kinetic evaluation of organic disinfection by-product and assimilable organic carbon (AOC) formation during the ozonation of drinking water. *Water Res.* **2006**, *40* (12), 2275–2286.

(88) Phungsai, P.; Kurisu, F.; Kasuga, I.; Furumai, H. Changes in dissolved organic matter composition and disinfection byproduct precursors in advanced drinking water treatment processes. *Environ. Sci. Technol.* **2018**, *52* (6), 3392–3401.

(89) Gan, W.; Huang, S.; Ge, Y.; Bond, T.; Westerhoff, P.; Zhai, J.; Yang, X. Chlorite formation during ClO_2 oxidation of model compounds having various functional groups and humic substances. *Water Res.* **2019**, *159*, 348–357.

(90) Skibinski, B.; Uhlig, S.; Müller, P.; Slavik, I.; Uhl, W. Impact of different combinations of water treatment processes on the concentration of disinfection byproducts and their precursors in swimming pool water. *Environ. Sci. Technol.* **2019**, *53* (14), 8115–8126.

(91) Xu, J.; Kralles, Z. T.; Dai, N. Effects of sunlight on the trichloronitromethane formation potential of wastewater effluents: Dependence on nitrite concentration. *Environ. Sci. Technol.* **2019**, *53* (8), 4285–4294.

(92) Li, C.; Wang, D.; Xu, X.; Wang, Z. Formation of known and unknown disinfection by-products from natural organic matter fractions during chlorination, chloramination, and ozonation. *Sci. Total Environ.* **2017**, *587–588*, 177–184.

(93) Maizel, A. C.; Remucal, C. K. Molecular composition and photochemical reactivity of size-fractionated dissolved organic matter. *Environ. Sci. Technol.* **2017**, *51* (4), 2113–2123.

(94) Gligorovski, S.; Strekowski, R.; Barbati, S.; Vione, D. Environmental implications of hydroxyl radicals ($^{\bullet}OH$). *Chem. Rev.* **2015**, *115* (24), 13051–13092.

(95) Young, T. R.; Li, W.; Guo, A.; Korshin, G. V.; Dodd, M. C. Characterization of disinfection byproduct formation and associated changes to dissolved organic matter during solar photolysis of free available chlorine. *Water Res.* **2018**, *146*, 318–327.

(96) Chen, M.; Kim, S.; Park, J.-E.; Jung, H.-J.; Hur, J. Structural and compositional changes of dissolved organic matter upon solid-phase extraction tracked by multiple analytical tools. *Anal. Bioanal. Chem.* **2016**, *408* (23), 6249–6258.

(97) Ohno, T.; He, Z.; Sleighter, R. L.; Honeycutt, C. W.; Hatcher, P. G. Ultrahigh resolution mass spectrometry and indicator species analysis to identify marker components of soil- and plant biomass-derived organic matter fractions. *Environ. Sci. Technol.* **2010**, *44* (22), 8594–8600.

(98) Zhang, H.; Zhang, Y.; Shi, Q.; Ren, S.; Yu, J.; Ji, F.; Luo, W.; Yang, M. Characterization of low molecular weight dissolved natural organic matter along the treatment train of a waterworks using Fourier transform ion cyclotron resonance mass spectrometry. *Water Res.* **2012**, *46* (16), 5197–5204.

(99) Rosario-Ortiz, F. L.; Canonica, S. Probe compounds to assess the photochemical activity of dissolved organic matter. *Environ. Sci. Technol.* **2016**, *50* (23), 12532–12547.

(100) Du, Y.; Wu, Q.-Y.; Lv, X.-T.; Ye, B.; Zhan, X.-M.; Lu, Y.; Hu, H.-Y. Electron donating capacity reduction of dissolved organic matter by solar irradiation reduces the cytotoxicity formation potential during wastewater chlorination. *Water Res.* **2018**, *145*, 94–102.

(101) Wenk, J.; Aeschbacher, M.; Salhi, E.; Canonica, S.; von Gunten, U.; Sander, M. Chemical oxidation of dissolved organic matter by chlorine dioxide, chlorine, and ozone: Effects on its optical and antioxidant properties. *Environ. Sci. Technol.* **2013**, *47* (19), 11147–11156.

(102) Lavonen, E. E.; Gonsior, M.; Tranvik, L. J.; Schmitt-Kopplin, P.; Köhler, S. J. Selective chlorination of natural organic matter: Identification of previously unknown disinfection byproducts. *Environ. Sci. Technol.* **2013**, *47* (5), 2264–2271.

(103) Kundu, B.; Richardson, S. D.; Granville, C. A.; Shaughnessy, D. T.; Hanley, N. M.; Swartz, P. D.; Richard, A. M.; Demarini, D. M. Comparative mutagenicity of halomethanes and halonitromethanes in Salmonella TA 100: Structure activity analysis and mutation spectra. *Mutat. Res., Fundam. Mol. Mech. Mutagen.* **2004**, *554* (1–2), 335–350.

(104) Plewa, M. J.; Wagner, E. D.; Mueller, M. G.; Hsu, K. M.; Richardson, S. Comparative mammalian cell toxicity of N-DBPs and C-DBPs: Occurrence, formation, health effects, and control of disinfection by-products in drinking water. In *Disinfection By-Products in Drinking Water*; Karanfil, T., Krasner, S. W., Westerhoff, P., Xie, Y., Eds.; 2008; p 36.

(105) Zhao, Q.; Shang, C.; Zhang, X.; Ding, G.; Yang, X. Formation of halogenated organic byproducts during medium-pressure UV and chlorine coexposure of model compounds, nom and bromide. *Water Res.* **2011**, *45* (19), 6545–6554.

(106) Page, S. E.; Arnold, W. A.; McNeill, K. Terephthalate as a probe for photochemically generated hydroxyl radical. *J. Environ. Monit.* **2010**, *12* (9), 1658–1665.

(107) Sharpless, C. M.; Aeschbacher, M.; Page, S. E.; Wenk, J.; Sander, M.; McNeill, K. Photooxidation-induced changes in optical, electrochemical, and photochemical properties of humic substances. *Environ. Sci. Technol.* **2014**, *48* (5), 2688–2696.

(108) Yang, M.; Zhang, X. Comparative developmental toxicity of new aromatic halogenated DBPs in a chlorinated saline sewage effluent to the marine polychaete *Platynereis dumerilii*. *Environ. Sci. Technol.* **2013**, *47* (19), 10868–10876.

(109) Mercier Shanks, C.; Sérodes, J.-B.; Rodriguez, M. J. Spatio-temporal variability of non-regulated disinfection by-products within a drinking water distribution network. *Water Res.* **2013**, *47* (9), 3231–3243.

(110) Allard, S.; Tan, J.; Joll, C. A.; von Gunten, U. Mechanistic study on the formation of $Cl^-/Br^-/I^-$ trihalomethanes during chlorination/chloramination combined with a theoretical cytotoxicity evaluation. *Environ. Sci. Technol.* **2015**, *49* (18), 11105–11114.

(111) Huang, K.; Shah, A. D. Role of tertiary amines in enhancing trihalomethane and haloacetic acid formation during chlorination of aromatic compounds and a natural organic matter extract. *Environ. Sci. Water Res. Tech* **2018**, *4* (5), 663–679.